In-wall Thermoelectric Harvesting for Wireless Sensor Networks

Aristotelis Kollias and Ioanis Nikolaidis
Computing Science Department, University of Alberta, Edmonton, T6G 2E8, Alberta, Canada

Keywords: Wireless Sensor Networks, Energy Harvesting, Thermoelectric Energy.

Abstract: We propose the use of embedded in-wall thermoelectric harvesters to power nodes of a wireless sensor network. We exploit the significant temperature differences between indoor and outdoor environments in cold climates. We use heat flow measurements of the exterior (outside-facing) wall of a number of apartments from the same apartment complex. We report on the degree of variability as well as on the seasonal changes that characterize the heat flow, and hence the potential for thermoelectric energy harvesting. We also examine whether the difference between indoor and outdoor air temperature is a good proxy for to the observed heat flow through the walls. Examples of data carrying capability of a particular harvester and sensor node combination are also provided.

1 INTRODUCTION

Wireless sensors are used to assist in structure maintenance (Vullers et al., 2010), to monitor human activity, to help prevent disasters like forest fires, and, in general, to collect data for scientific and business purposes. In the construction industry, sensors can be used to alert of dangerous situations, in cases where the infrastructure is critically compromised and to monitor wear and the "health" of buildings in general. For example, humidity sensors inside wall structures can provide advance warning of excess humidity which could lead to toxic mould growth, and strain dynamometers sensors can be used to determine the response of the building during earthquakes.

We consider the standard model for wireless sensor network (WSN) nodes, i.e., as consisting of a transceiver, the sensor, a microcontroller and an energy source, usually a battery. Generally, when the energy source for the WSN node is a battery, there exists a limit to how long the node can function without servicing, i.e., changing of batteries. With current technology, the node modules generally exhibit low energy consumption, therefore the lifetime limit that a battery imposes can be long enough that, depending on the situation, replacing batteries will not impose a significant cost. However, in particular situations, the sensors are inaccessible, i.e., embedded within structures, like walls, and the cost of replacing the energy source might be prohibitive.

There are three possible solutions for difficult–to-access sensor nodes. They can be either abandoned after they have performed their function for some time (with the hope that other, nearby, sensors will take over the task of measuring the same phenomenon), or they can be all connected to a wired power distribution subsystem. Finally, energy harvesting could be employed. Abandoning the sensors is an expensive option and possibly unacceptable. The wiring option is expensive in terms of labor cost and materials, exacerbated by the ever increasing price of copper, and wiring defeats the advantage of using wireless, since communication can be accomplished over the same wires that provide power. Wiring also results in a structure which is more complex and could be prone to faults (accidental puncture/cutting of the wires, problems with single points of failure, collection of RF energy by acting as low frequency antennas, etc.). In short, the ability of each node to power itself from energy harvesting leads to better node autonomy, and overall system resilience.

The solution adopted in this paper is to use thermoelectric energy harvesters to power each sensor node. Energy harvesters exploit the ambient energy of the environment to replenish the energy stored in the battery or the super capacitor. Photovoltaic harvesters have been studied extensively in previous works e.g., (Gorlatova et al., 2011). Buildings with good illumination can use photovoltaic energy to power sensor modules. Instead, in this paper we consider thermoelectric energy harvesting because (a) the potential for photovoltaic energy can be limited due to sub-optimal

Kollias A. and Nikolaidis I..
In-Wall Thermoelectric Harvesting for Wireless Sensor Networks.
DOI: 10.5220/0004864102130221
In *Proceedings of the 3rd International Conference on Smart Grids and Green IT Systems* (SMARTGREENS-2014), pages 213-221
ISBN: 978-989-758-025-3

placement, and because of long nights, as is the case at latitudes of northern continental climates, while, (b), during winter the indoor to outdoor temperature difference can reach as much as 60 degrees Celsius creating unparalleled opportunities for thermoelectric harvesting. More specifically, we take advantage of the difference between indoor and outdoor temperature in buildings in northern climates. To this end, we use data collected from an actual inhabited apartment complex in Fort McMurray, Alberta, Canada. The particular apartment complex has been constructed using modular construction techniques.

Placing thermoelectric harvesters inside walls serves the application of powering co-located sensors that monitor the wall and building behaviour. In climates like the one considered in our study, extreme weather conditions can cause events important to the integrity of a building, e.g., breakage of water pipes, more frequently occurring than in moderate climates. The ability to embed sensors in inaccessible locations that autonomously operate for several decades (i.e., as long as the building lasts), monitoring for such events, can currently only be supported using energy harvesting.

In terms of the methodology followed, we use the difference between indoor air and outdoor air temperature as the basis for the energy harvesting potential we report in this paper. Nevertheless, the energy harvesting specific to an apartment (and, more specifically, to a location on an exterior wall of an apartment) depends on a number of factors whose combined effect can be captured by the heat flow rate through specific locations of the exterior walls. We therefore study whether the difference between indoor and outdoor temperature at each apartment is a good proxy for the actual heat flow via the exterior walls. The heat flow is the real rate of energy transfer via the wall unit, i.e., the ground truth. Our study indicates among other things that, even though the difference between indoor and outdoor air temperature is a good (scaled) proxy for the average heat flow, there exists a high degree of variability of heat flow across apartments. Furthermore, the variability is smaller during certain times of the year. We comment on how these observations should guide the design of suitable network protocols.

The remaining of the paper is structured as follows. Section 2 briefly reviews some related work on the subject at hand, Section 3 has the description of the data set, and elements of the methodology we followed in interpreting them. Section 4 outlines the system model that we employ. Section 5 presents numerical performance results. We conclude with Section 6 summarizing our findings.

2 RELATED WORK

Energy harvesting for wireless networks and low power wireless sensor node architectures are areas of intense research activity. The use of energy harvesting for powering WSN nodes, with example applications, such as smart buildings and predictive maintenance of structures has been explored in the past (Vullers et al., 2010).

In this paper we narrow our focus to thermoelectric generators and specifically exploit the energy lost through walls in cold climates. We use a device model loosely based on (Mateu et al., 2006), in which energy harvesting from the human body was used, which is an idea explored by other researchers as well, (Ramadass and Chandrakasan, 2011; Wang et al., 2009). The devices proposed in previous works assume operation based on the difference of temperature between the human body and its environment, thus indirectly exploiting the temperature homeostasis of the human body.

In this paper, we are not concerned with the task of increasing the energy harvesters efficiency, a topic of intense activity anyway, e.g., (Hudak and Amatucci, 2008; Luber et al., 2013). We use off-the-shelf components and we do not even use a sensor platform optimized for energy efficiency. In other words, the results we present here are very close to representing a "worst case" scenario with respect to the devices employed.

In the field of energy harvesting for WSNs, a notable work is that of Gorlatova et al. (Gorlatova et al., 2009; Gorlatova et al., 2011) which focuses on how to use photovoltaic harvesting under diverse use scenarios, by proposing suitable optimization models. Another distinct property of their work is the study of photovoltaic harvesting in environments under the control of the users (depending on indoor illumination, or in the pocket of users), i.e., with idiosyncratic and sometimes unpredictable behaviour. They also consider elementary WSN applications, such as ID beacon transmission.

3 THE DATA SET

We use data collected over a period of a year, from 11 different apartments within a single apartment complex in Fort McMurray, Alberta, Canada. The data collected is comprehensive, including such aspects as water flow and temperature for the water used by radiators for heating, water flow and temperature for residential water, CO2 concentration, etc. For the purposes of this study we consider only the heat flow

through exterior (outside-facing) walls, the indoor air temperature, and the outdoor air temperature. The data collection was conducted in real–time and is still taking place, but we extract a one year period (8th of September of 2012 to the 8th of September of 2013) which is sufficient for the purposes of capturing seasonal variations.

In our data set, we obtain a separate indoor air temperature for each apartment but have a single outdoor air temperature, as acquired by the Building Automation System (BAS). It has to be noted that a single outdoor air temperature is, again, only an approximation of the locally specific outdoor wall temperature of each wall unit, since phenomena like convection can, depending on airspeed, result in different temperatures at different spots and orientations.

The heat flow measurements are obtained at two locations (one on a stud, and one on the insulation) of the exterior–facing wall of each apartment. Of the two heat flow measurements the one most relevant to our study, which we subsequently use, is the heat flow via the stud. Studs are necessary for the structure and proper framing of the walls but at the same time they are responsible for loss of heat as they represent a "bridge" of smaller thermal resistance (compared to the insulated area of the wall) between interior and exterior.

3.1 The Methodological Approach

The heat flow through a wall reflects the combined results of wall construction qualities (stud spacing, insulation, etc.), of human activity (e.g. the choice of thermostat setpoints, opening of windows, etc.), of weather phenomena (temperature, wind direction, etc.), the particular orientation and location of the apartment, and of course the exact location of the sensor in the wall. As we will see, the combination of the factors leads to a highly variable heat flow which nevertheless exhibits distinct seasonal characteristics.

We use heat flow data to describe the extent to which thermoelectric energy harvesting through the exterior walls is adequate to power (and to what degree) WSN nodes. Heat flow (measured in W/m^2 units) through exterior walls is directly related to the temperature difference between the two sides of the wall. Heat flow through an infinitesimally narrow slice of surface is defined as, $\vec{q} = -k\nabla T$ where $\vec{q}$ is the local heat flow, k is the materials heat conductivity and ∇T is the temperature gradient. We note that heat flow is a vector. We use the convention that a positive heat flow represents loss of heat (i.e., radiating from the interior side of the wall to the exterior side) while a negative indicates the reverse direction. Naturally, due to the climate characteristics in Fort McMurray, the latter case is infrequent, and occurs almost exclusively during the warmest summer months.

More precisely, if the wall is to be treated as a single homogeneous material of infinite area and thickness L the heat flow is inversely proportional to the thickness, that is, $\vec{q} = -kL^{-1}\nabla T$. In reality, the walls are more complex non-homogenous structures containing cavities, insulation, studs for wall support, studs for window framing, etc. impacting collectively on the heat flow magnitude and direction.

The thermoelectric harvesters are also dependent on the temperature differences to produce electricity and their output is governed by $-\nabla V = S\nabla T$ where S is the Seebeck coefficient of the material and ∇V is the electric potential between the two harvester terminals. In Section 5 we correlate the heat flux data (q_{hf}) with the air temperature difference between indoor and outdoor (ΔT_{air}).

After establishing a strong relation between q_{hf} and ΔT_{air}, we subsequently use ΔT_{air} as a proxy of the actual temperatures of the two (inside and outside) wall surfaces. This is primarily because the air temperature represents averages whereas q_{hf} is specific to the location of the wall where the heat flow sensor is mounted. However, our reasoning is that any thermal harvester installed in the wall will experience similar heat transfer behaviour as the heat flow sensors measure at the same location. Hence, whereas ΔT_{air} is a good basis for an overall estimate of energy harvesting potential, regardless of where the harvester is placed on the exterior wall, q_{hf} allows us to examine the highly idiosyncratic behaviour (captured by the standard deviation) due to the factors we listed at the beginning of this section.

Our interest in ΔT_{air} and q_{hf} and their relation is also motivated by the intention to use, in a future design, a thermoelectric harvester inside the wall whose two sides are in contact to the two wall surfaces via materials of high thermal conductivity, e.g., metal. This would allow the thermal harvester to be a low thermal resistance "bridge" and hence receive the full potential of the temperature difference of the two surfaces. However, such a design is future work because it needs to satisfy several other structural, mechanical, and safety constraints for in-wall embedding.

4 THE DEVICE MODEL

4.1 The Harvester Model

Our model is based on the performance of the TEC1-12703 Peltier module. The module has a surface area

of 16 cm^2. We carried out characterization experiments to determine the relation between ΔT and energy harvested. The setup was a small "refrigerator", using TEC1-12703 modules (see Figure 1), arranged such that, a constant ΔT was created and the resulting energy harvested measured. This refrigerator is made by using (top to bottom): (i) a heat sink, which is connected to a TEC1-12703, also connected to a power supply, to provide the hot side temperature for the harvester, (ii) the harvester, with its other side connected to, (iii) another TEC1-12703 module, again connected to the power supply to provide the cold side temperature. Lastly, another heat sink along with a small fan was used to help regulate the heat and stabilize ΔT. This setup was used to maintain constant ΔT ranging up to 40 degrees Celsius. The temperatures were sensed using thermistors, and a separate sensor module. Our findings indicate that the power output, W (in mW), of the particular harvester relates to ΔT (in Celsius) as $W = (2.57\ \Delta T^2 + 5.88\ \Delta T + 0.11) \cdot 10^{-3}$ (Least Squares fit with $R^2 = 0.9358$).

4.2 The Sensor Model

In order to develop a WSN node energy consumption model, we use the NanoZ-CC2530 device which employs the TI CC2530 microcontroller. We operate it with another node acting as data sink, communicating using the z-stack tool (ti.com, 2012) (Zigbee compliant). We carried out energy-exhaustion tests to determine for how long (how many bytes) of *payload* can be transmitted for the amount of energy accumulated to sufficiently charge a 1 Farad capacitor (rated at 5 V) up to 3.6 V. The packets transmitted followed the standard Zigbee data frame structure. We first conducted experiments using the TEC1-12703 harvester connected to a Texas Instruments BQ25504 Evaluation Board to regulate the voltage and to determine the ability of the harvester to charge the capacitor. After the success of the first step, and in the interest of accelerating the experiments, we used a standard power supply (GPC-3030) to charge the capacitor to the same 3.6 V. The capacitor was then connected to the NanoZ module and used to send data until exhaustion. From the measurements we concluded that it was possible to transmit an average of 4103.7 bytes of payload per Joule using messages of maximum payload size (90 bytes per packet). The sensor modules are not energy efficient, as we measured that they consume 0.49 mW in their sleep state when the processor is set to the sleep mode PM2 (only low-frequency oscillator operating), of which only approximately 6 μW is due to the processor consumption (as per the processor datasheet).

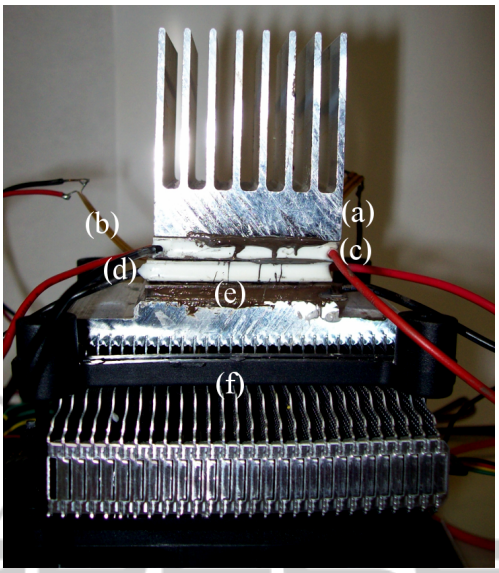

Figure 1: The harvester experimental setup. Shown in the figure are: (a) heat sink for temperature control of the "hot side", (b) thermistor for measuring the "hot side" temperature, (c) thermoelectric heater for the hot side, (d) the thermoelectric harvester, (e) the same as (c) but for generating the "cold side" temperature, (f) fan with heat sink for thermal control of the "cold side".

Table 1: Correlation of ΔT_{air} and q_{hf}.

Apartment	$corr(\Delta T_{air}, q_{hf})$
1	0.86
2	0.93
3	0.90
4	0.82
5	0.81
6	0.88
7	0.85
8	0.91
9	0.84
10	0.86
11	0.84

5 NUMERICAL RESULTS

We first consider the correlation of the ΔT_{air} and q_{hf} time series over the entire year and separately for each apartment. The time series represent hourly averages of the respective values. Table 1 demonstrates the overall strong correlation of the two time series but there exist differences (e.g. 0.93 for apartment 2 and 0.82 for apartment 4) that are ultimately related to the occupant(s) actions and behaviour. To illustrate the nature of differences consider the scatterplots of ΔT_{air} and q_{hf} in Figure 3 and 4 for the entire year, showing an overall strong correlation but with significant

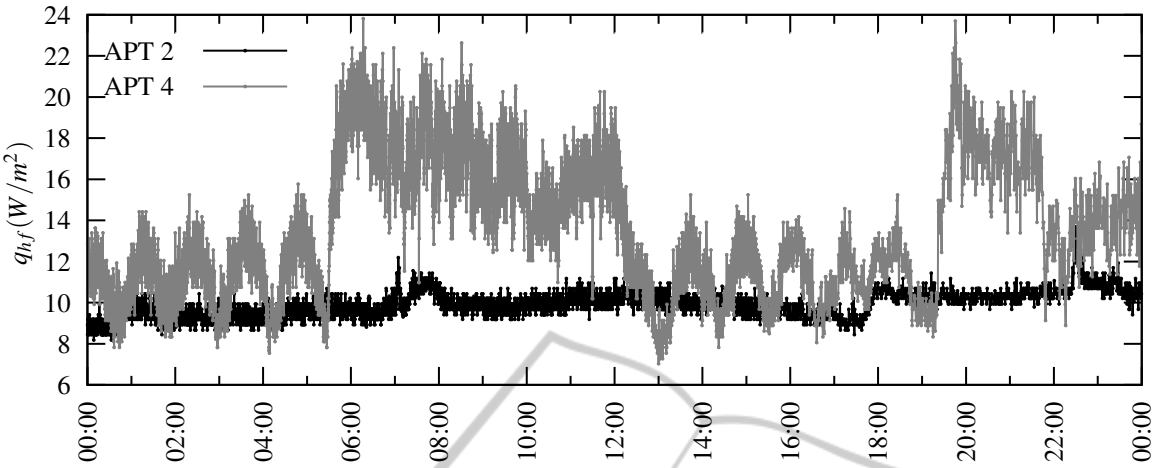

Figure 2: Intra-day q_{hf} in apartments 2 and 4.

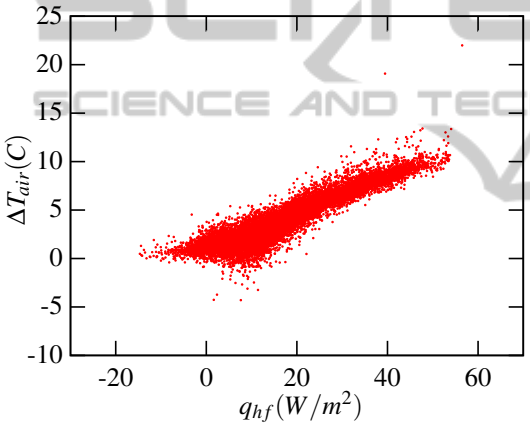

Figure 3: Apartment 2 ΔT_{air} vs. q_{hf}.

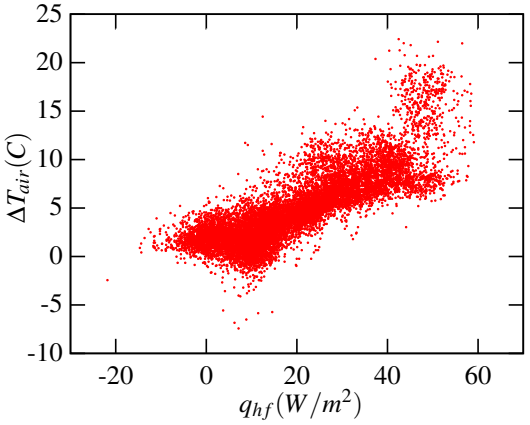

Figure 4: Apartment 4 ΔT_{air} vs. q_{hf}.

variance and occasional outlier points.

Without precisely knowing the inhabitants behaviour, one can only conjecture on several reasons for certain outliers (the resident could have been using an electrical radiator close to the location of the heat flow sensor, or touching the wall at the sensor location, or had the windows open, etc.). To illustrate the differences that might show up, consider Figure 2 showing the heat flow during a specific day (in mid-March of 2013) during which one of the two presented apartments had almost constant heat flow (possibly the apartment was vacant that day) while the other one had highly variable heat flow (the oscillations are probably due to the heating cycling around the thermostat setpoint, while higher setpoints and possible resident activity are evident from approximately 6am to 12pm and from approximately 8pm to 10pm).

We define $s^{(d)}_{avg}$, $s^{(d)}_{max}$, and $s^{(d)}_{min}$ as, respectively, the average, maximum, and minimum of daily q_{hf} standard deviation, calculated based on the hourly measurements of each day. Essentially we try to capture the statistics of variability of q_{hf} within the same day as they behave across the year. As can be seen from Table 2 the remarkable fact is that there exist days that almost every apartment shows a drastically small standard deviation. Apartments 3 and 4 exhibit a $s^{(d)}_{min}$ of 0.18 and even the apartment 11 which has the largest intra-day standard deviation of 8.37 still has low variability days as its $s^{(d)}_{min}$ of 0.37 illustrates. Our current conjecture is that the days of low variability represent days that the apartments were possibly vacant, and hence no resident–related influence was introduced apart from leaving the thermostat at a particular (and possibly low) setpoint.

Next, we try to capture the differences across groups of apartments based on the floor and their orientation. To this end, we define $\sigma^{(y)}_{avg}$, $\sigma^{(y)}_{max}$ and $\sigma^{(y)}_{min}$, representing, respectively, the average, maximum and

Table 2: q_{hf} and its standard deviation for various apartments, and potential harvesting output.

Apt.	$avg.q_{hf}$	$s^{(d)}_{avg}$	$s^{(d)}_{max}$	$s^{(d)}_{min}$	harvested (mW)	bytes/day
1	7.19	1.70	5.17	0.31	2.15	761864(588130)
2	5.91	0.98	2.76	0.19	1.74	617129(443395)
3	8.31	1.82	5.76	0.18	2.58	916274(742539)
4	6.80	2.06	6.42	0.18	2.06	730854(557119)
5	6.50	1.84	6.55	0.34	2.30	815768(642034)
6	8.25	2.64	7.20	0.41	2.23	790079(616345)
7	5.61	2.46	6.77	0.48	2.11	747428(573694)
8	8.07	1.40	4.15	0.26	2.45	870314(696580)
9	7.30	2.74	5.79	0.29	2.28	809130(635396)
10	6.85	3.24	7.99	0.42	2.06	730610(556876)
11	7.18	2.15	8.37	0.37	1.91	675688(501954)

minimum of the standard deviation of the daily averages of particular groupings of apartments across the entire year. Table 3 (ε stands for a quantity less than 0.005) provides some interesting results. As expected, by comparing to Table 2, the overall variability is less pronounced at the larger time scale of a year as it dilutes the effects of intra-day variance seen in Table 2. While the maximum variability, i.e., $\sigma^{(y)}_{max}$, can still reach significant levels, it is less than the one observed intra–day.

The minimum, $\sigma^{(y)}_{min}$, reaches a small value which occurs during summer days when the outdoor and indoor temperatures are almost equal and the temperature across all apartments is similar as well. Unfortunately, less variable days across apartments are also days of small harvesting potential because ΔT is small. Furthermore, due to the occupant behaviour, we encounter cases such as the average q_{hf} at floor 3 and 4 being quite different (6.66 vs. 7.41). The implication of this observation is that, should multi-hop forwarding be used in the sensor nodes, the bottleneck (in terms of nodes with least harvested energy) could assume undesirable topological characteristics, by restricting the paths that could be followed to collect the data to sink nodes. In this example, an entire floor may not have enough energy to forward traffic between adjacent floors, towards a sink node placed at the bottom floor.

Despite the variability, seasonal patterns are evident across all apartments. Consider for example Figure 5 which shows the differences of two apartments (number 2 and 4) over the entire year. Indeed, even though the differences on certain days can be significant, they follow identical seasonal trends. The trends are also similar to all the other apartments (not shown here for the sake of brevity).

Finally, we note that there exist relatively important differences in the heat flow, and hence on harvesting potential, between night and day. To put it differently, the amount of energy collected in the morning hours is generally different from what could be collected overnight. Therefore, the intra–day variability could be handled by collecting energy over an entire (and possibly more than one) day, modulo of course the seasonal variations. For the night vs. day differences, we present the, rather arbitrarily chosen, intervals of day (6am to 6pm) and night (6pm to 6am). Hence, each day represents two (average) measurements. When considered in groupings of weeks, and across all weeks of the year, we produce Table 4 where we can readily see the ratio between maximum and minimum standard deviation can be significant and it is not uncommon to find a 5-times difference (apartment 6 is a good example with maximum over a week of 4.09 and minimum over another week of 0.77). Extending the averaging over a longer time scale will naturally smooth the variability extremes. For example, in Table 5, each entire day is represented by its average value, and the standard deviation of the daily measurements over a month (defined as a sequence of 30 days) are reported, across the entire year. The maximum variability is tamed but the difference between minimum and maximum standard deviation of the same apartment can still be surprisingly large (apartment 6 has a maximum of 3.09 and a minimum of only 0.30).

Table 3: Average q_{hf} vs. orientation/elevation.

	$avg.q_{hf}$	$\sigma^{(y)}_{avg}$	$\sigma^{(y)}_{max}$	$\sigma^{(y)}_{min}$
Orientation				
North	7.00	0.95	3.08	0.17
South	7.14	0.78	3.04	0.24
Elevation				
1st floor	7.05	0.25	4.19	ε
2nd floor	7.22	0.78	3.57	0.11
3rd floor	6.66	0.74	3.02	0.03
4th floor	7.41	1.06	4.18	0.02

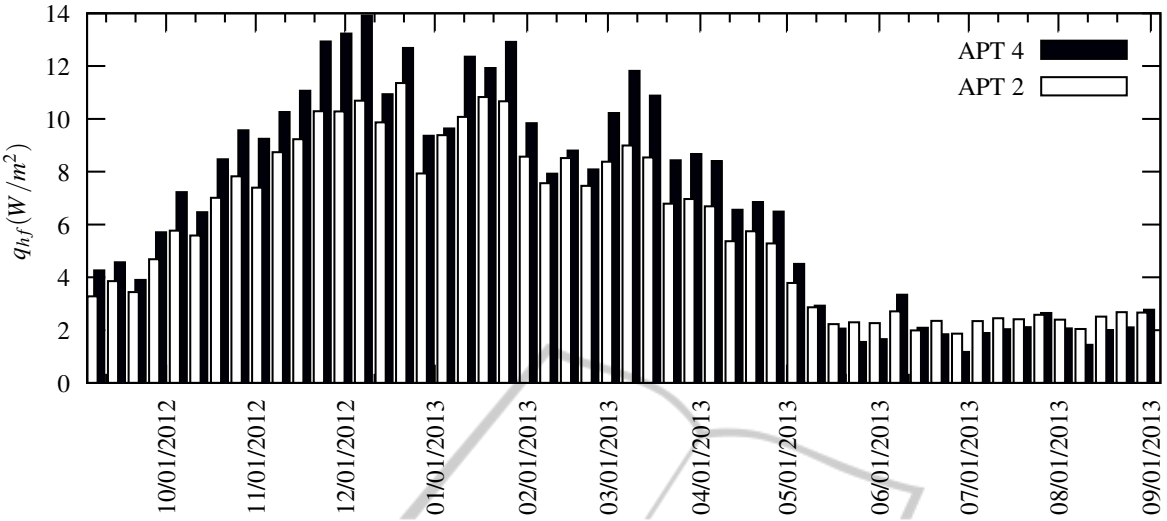

Figure 5: Daily average q_{hf} in apartments 2 and 4.

Table 4: Average, maximum and minimum weekly standard deviation of q_{hf}.

Apt.	$s^{(w)}_{avg}$	$s^{(w)}_{max}$	$s^{(w)}_{min}$
1	1.25	2.28	0.48
2	0.87	1.51	0.29
3	1.51	3.21	0.37
4	1.50	3.17	0.49
5	1.24	3.25	0.47
6	1.97	4.09	0.77
7	1.38	2.31	0.49
8	1.37	2.79	0.49
9	1.93	2.91	0.79
10	1.97	3.54	0.70
11	1.53	3.17	0.61

Table 5: Average, maximum and minimum monthly standard deviation of q_{hf}.

Apt.	$s^{(m)}_{avg}$	$s^{(m)}_{max}$	$s^{(m)}_{min}$
1	1.40	2.27	0.81
2	0.93	1.57	0.40
3	1.52	2.44	0.68
4	1.44	2.34	0.62
5	1.17	1.79	0.35
6	1.89	3.09	0.30
7	1.44	2.17	0.44
8	1.47	2.36	0.48
9	1.80	2.61	0.18
10	1.99	2.76	1.22
11	1.57	2.65	0.62

5.1 Data Transfer Capabilities

Let us return to Table 2 and notice the harvested power potential using ΔT_{air} and the model of the harvester noted earlier. The average power that can be harvested in the apartments exterior wall is $2.17\,mW$ with a standard deviation of $0.22\,mW$. The highest average is $2.58\,mW$, and the apartment producing the lowest could harvest $1.74\,mW$. Assuming we harvest energy to transmit once a day, each node could transmit an average of approximately 770 kbytes of payload per day. The per-apartment potential daily transfer volume can be seen in Table 2. The numbers in parentheses are the payload that could be transmitted per day assuming at all other times the sensor node idles as described in the node model, i.e., consuming $0.49\,mW$ in its sleep state. Admittedly, much better performance is possible with better designed nodes. However, even at 600 kbytes of payload per day, a sensor can adequately send samples of its own sensing (e.g.. slowly changing humidity values or accelerometer activity compressed to the interesting events only) and still have some energy capacity to perform multi-hop routing.

However, as Figure 5 indicates, during the summer there might not be enough power to send data without risking an outage. Specifically, apartment 11 during the week of 6/29 to 7/5 was able to harvest only an average power of $0.113\,mW$, that is not sufficient to even power the sensor module. The exact sensor node design is also important. For example, assuming that an external circuit duty-cycles the operation of the entire node, then the restarting (equivalent to a cold boot) of the particular nodes we employed takes around 2 seconds to complete during which time it consumes the same power as when transmitting, $84.51\,mW$. After those 2 seconds the device en-

ters sleep mode where it consumes $0.49\,mW$. Hence, power-up is a costly overhead of $\sim 169.02\,mJoule$, and a strategy of repeatedly powering up on-demand to gather data (not even transmitting) is probably unacceptable. Or, equivalently, the particular sensor would have to harvest energy for an average of 1497 seconds, to just cope with the 2 seconds startup energy cost before it performed any useful sampling, computation, and transmission (energy permitting), thus limiting the rate of sampling/sensing.

If the energy storage capacity is small to allow the longer term harvesting, outage is almost certain during summer months. The particular apartments do not have air-conditioning units for cooling, as they are rarely used in such northern climates. Thermoelectric harvesting during the summer occurs mostly at night when the outside temperature drops.

The good news is that due to the significant variability across apartments and throughout the day, a protocol to determine, at least locally, which node has (or has had in the recent past) the good fortune of harvesting more energy could be suitable for routing. In other words, there indeed exists diversity of opportunities to spend energy of another neighboring node because of the corresponding diversity in inhabitant behaviour. As a rule though, such routing strategies must become more conservative during the summer when the harvesting potential is reduced in both absolute numbers and in terms of variability across apartments. Our recommendation would therefore be in favour of "seasonally-aware" routing algorithms.

The potential of photovoltaic output from a cell of the same surface area ($16\,cm^2$) as the thermoelectric harvester used, at the same geographical location, and using off-the-shelf solar cells with efficiency 17% on a south-facing vertical wall is an average daily power of $88.739\,mW$ (according to data in Natural Resources Canada website (pv.nrcan.gc.ca, 2013). The average power from thermoelectric harvesting appears low by comparison. However, one has to consider that (1) the solar power favors the south facing side of the building, over the north facing ones, and (2) to harvest solar energy the placement of the photovoltaic cells is crucial and one has to consider problems of occlusion of the light source, compared to a fairly flexible placement of the thermoelectric harvesters. Finally, as a matter of aesthetics, a photovoltaic harvester requires that it be exposed to outside view, whereas a thermoelectric harvester can be embedded "out of sight" within the wall structures.

6 CONCLUSIONS

In anticipation of deploying in-wall wireless sensors for structure monitoring this paper reports measurements of temperature difference and heat flux taken in an apartment building at Fort McMurray, Alberta, to evaluate the feasibility of using thermoelectric energy harvesting in cold northern climates. We conclude that the use of such harvesters for wireless sensor modules is possible with current technology albeit not without some challenges.

First, even though the difference between indoor and outdoor air temperature is a good proxy for the potential energy harvesting, the exact behaviour of heat flow that ultimately governs the thermoelectric harvesting at particular points of the wall structure are subject to factors that are dependent on weather phenomena (e.g., convection phenomena on the wall surfaces) but, more importantly, on the behaviour patterns of the residents who are in control of not only the thermostat setpoints but also of objects attached to or close to the walls, extra forms of directional heat radiators (e.g. electric heaters), and so on.

Second, even though the heat flow follows, as expected, a seasonal pattern, its variability from one outside wall to another (one apartment to another) can be significant, especially when observed in small time scales, e.g., intra-day. Hence, despite the regularity of the harvesting potential, it is to be expected even within the same day, that the wall on some apartments can sustain higher volume of sensor data transfers than others. The implications of this behaviour to multi-hop routing are obvious. Short-term alternative routing paths would need to be considered.

Finally, the harvesting potential is reduced in the summer months and appears possible almost exclusively later in the day. Additionally, in the summer months, the variability of harvesting becomes smaller. Hence, sizing the energy storage (e.g., capacitance of a supercapacitor) necessary to sustain the sensor node operations, should be based on the worst case summer harvesting potential. One could argue that we need to consider complementing thermoelectric harvesting with photovoltaic harvesting which reaches its peak output during the summer months. Nevertheless, such a decision is dependent on a decision to expose the photovoltaic element which we try to completely avoid as we wish to deploy the sensors as inconspicuously as possible.

We are currently working towards a modular design for simple in-wall placement.

ACKNOWLEDGEMENTS

The authors would like to thank the funding support of the Natural Sciences and Engineering Research Council of Canada (NSERC) through a CRD Grant and the invaluable technical assistance of Mrs. Veselin Ganev and Jianfeng Dai.

REFERENCES

Gorlatova, M., Kinget, P., Kymissis, I., Rubenstein, D., Wang, X., and Zussman, G. (2009). Challenge: ultra-low-power energy-harvesting active networked tags (enhants). In *Proceedings of the 15th annual international conference on Mobile computing and networking*, pages 253–260. ACM.

Gorlatova, M., Wallwater, A., and Zussman, G. (2011). Networking low-power energy harvesting devices: Measurements and algorithms. In *INFOCOM, 2011 Proceedings IEEE*, pages 1602–1610.

Hudak, N. S. and Amatucci, G. G. (2008). Small-scale energy harvesting through thermoelectric, vibration, and radiofrequency power conversion. *Journal of Applied Physics*, 103(10):101301–101301.

Luber, E. J., Mobarok, M. H., and Buriak, J. M. (2013). Solution-processed zinc phosphide (α-zn3p2) colloidal semiconducting nanocrystals for thin film photovoltaic applications. *ACS nano*, 7(9):8136–8146.

Mateu, L., Codrea, C., Lucas, N., Pollak, M., and Spies, P. (2006). Energy harvesting for wireless communication systems using thermogenerators. In *Proceeding of the XXI Conference on Design of Circuits and Integrated Systems (DCIS), Barcelona, Spain*.

pv.nrcan.gc.ca (2013). Photovoltaic potential and solar resource maps of canada. http://pv.nrcan.gc.ca/index.php?n=794&m=u&lang=e. [Online; accessed January 2014].

Ramadass, Y. and Chandrakasan, A. (2011). A battery-less thermoelectric energy harvesting interface circuit with 35 mv startup voltage. *Solid-State Circuits, IEEE Journal of*, 46(1):333–341.

ti.com (2012). A fully compliant zigbee 2012 solution: Z-stack. http://www.ti.com/tool/z-stack. [Online; accessed January 2014].

Vullers, R. J., Schaijk, R., Visser, H. J., Penders, J., and Hoof, C. V. (2010). Energy harvesting for autonomous wireless sensor networks. *Solid-State Circuits Magazine, IEEE*, 2(2):29–38.

Wang, Z., Leonov, V., Fiorini, P., and Van Hoof, C. (2009). Realization of a wearable miniaturized thermoelectric generator for human body applications. *Sensors and Actuators A: Physical*, 156(1):95–102.